







# An Interpretable Machine Learning Model for Meningioma Grade Prediction

Ali Golbaf<sup>1</sup><sup>a</sup>, Damjan Veljanoski<sup>2</sup><sup>b</sup>, Prutha Chawda<sup>2</sup><sup>c</sup>, Swen Gaudl<sup>1</sup><sup>d</sup>,  
C. Oliver Hanemann<sup>2</sup><sup>e</sup> and Emmanuel Ifeakor<sup>1</sup><sup>f</sup>

<sup>1</sup>*School of Engineering, Computing and Mathematics, University of Plymouth, Plymouth, U.K.*

<sup>2</sup>*Peninsula Schools of Medicine, University of Plymouth University, Plymouth, U.K.*

**Keywords:** Meningiomas, Grading, Radiomics, MRI, Interpretable Techniques.


**Abstract:** Accurate preoperative prediction of meningioma grade is crucial for enhancing the clinical management of these tumours. In this study, we developed a non-invasive machine learning (ML) model to predict meningioma grade using clinical features and radiomics features from preoperative MRI scans, focusing on interpretability to improve clinical adoption of such models. A dataset of 94 patients from The Cancer Imaging Archive (TCIA) was analysed. Clinical features and radiomics features from T1-weighted contrast-enhanced (T1C) and T2-weighted Fluid Attenuated Inversion Recovery (T2 FLAIR) scans were utilised. Two feature subsets were constructed: one using radiomics features alone and the other combining clinical and radiomics features. Feature selection was performed using a modified Least Absolute Shrinkage and Selection Operator (LASSO) technique. Four ML models: Logistic Regression (LR), Support Vector Machine (SVM), Random Forest (RF), and Gradient Boosting (GB), were developed. SHapley Additive exPlanations (SHAP) was employed to address the blackbox nature of ML models by providing radiomics overall feature importance scores and model interpretation. Results using the clinical-radiomics subset showed that the SVM outperformed others (test AUC: 0.83), indicating its reliability for predicting meningioma grade. SHAP highlights discriminative radiomics features and their interaction with clinical features, thereby enhancing the clinical adoption of such models.


## 1 INTRODUCTION


Meningiomas, the most common primary brain tumours, are among the most understudied tumours within the central nervous system (Low et al. 2022). However, a significant proportion of meningiomas (20% - 30%), show aggressive behaviour, and high recurrence rate (Zhang et al. 2019). These tumours are categorised into three grades, according to 2021 World Health Organisation (WHO) guidelines (Louis et al. 2021). High-grade meningiomas (Grades II and III) show more aggressive behaviour than low-grade cases (Grade I), leading to a 5-year progression free survival probability (Wang, Nassiri, et al. 2023).


They are also challenging to be completely resected using invasive treatment strategies and often require adjunctive radiotherapy (Fountain, Young, and Santarius 2020). Thus, accurate grading of these tumours is important in enhancing the clinical management of meningiomas.


The gold standard for grading of meningiomas still relies on invasive methods such as histopathology and biopsy (Herrgott et al. 2023). However, invasive methods may not be applicable to tumours that are surgically inaccessible and patients with multiple diseases. Moreover, biopsies may not accurately reflect the heterogeneity of meningiomas due to limited sampling (Islim et al. 2020; Tagle et al.


<sup>a</sup> <https://orcid.org/0000-0002-8104-5600>

<sup>b</sup> <https://orcid.org/0000-0002-4951-8586>

<sup>c</sup> <https://orcid.org/0009-0004-0345-9017>

<sup>d</sup> <https://orcid.org/0000-0003-3116-3761>

<sup>e</sup> <https://orcid.org/0000-0002-1951-1025>

<sup>f</sup> <https://orcid.org/0000-0001-8362-6292>

2002). Consequently, there is a growing need for the development of non-invasive models that accurately predict the grade of meningiomas.

Currently, MRI serves as the primary non-invasive method in the clinical management of meningiomas (Zhang et al. 2020). However, some conventional MRI features of different meningioma grades overlap, which can potentially lead to misdiagnosis (Spille et al. 2019). In this context, radiomic, which is a quantitative approach for medical image analysis, has emerged as a novel way to extract imaging features that carry valuable biological information about tumours which are not accessible by conventional image analysis (Lambin et al. 2012). Machine learning has also demonstrated potential in developing non-invasive predictive models by capturing complex patterns within these features (Langs et al. 2018). Such models have been developed for the diagnosis, prognosis, and treatment of meningiomas, and have particularly shown promise in meningioma grading (Patel et al. 2023).

However, radiomics and machine learning have not yet been adopted in the clinical management of meningiomas. The blackbox nature of machine learning models make their outputs difficult to interpret (Patel et al. 2023). The application of interpretability techniques may mitigate the inherent blackbox nature of machine learning models (Reyes et al. 2020). However, only a few studies have focused on improving the interpretability of machine learning models in the clinical management of meningiomas. SHAP, which is used to assess the contribution of each radiomic feature to model performance, has been used to interpret a machine learning model for evaluating the post-surgical recurrence of high-grade meningiomas (Park, Choi, et al. 2022). Relevance-weighted Class Activation Mapping, an explanation method for visualising class relevance, has been employed to explain a machine learning model for meningioma segmentation (Jun et al. 2023). Additionally, Local Interpretable Model-Agnostic Explanations (LIME), an estimator technique, which approximates models locally for interpretability, has been applied to interpret machine learning models, for predicting glioma grades but not for the prediction of meningioma grade (Wang et al. 2019).

In this paper, we developed an interpretable machine learning model for predicting meningioma grade using both clinical and radiomics features. The aim is to enhance the adoption of radiomics and machine learning in the clinical management of meningiomas by establishing links between

meningioma grade, radiomics features, and their interactions with clinical features.

## 2 METHODS

### 2.1 Dataset

The dataset used in this study was obtained from TCIA, a publicly available database (Clark et al. 2013). It comprises a cohort of 96 patients who were diagnosed with meningioma between 2010 and 2019 (Vasantachart). Low-grade and high-grade meningiomas were identified according to the 2016 WHO guidelines. Clinical features were also recorded by two experienced neuropathologists and one neuropathology fellow. All patients underwent pre-operative T1C, and T2 FLAIR MRI scans. A detailed description of the imaging protocol can be found in (Vasantachart et al. 2022). In this study, cases with inconsistent histopathological records and suboptimal image qualities were excluded, yielding a final cohort of 94 patients. The clinical features of the patients are summarised in Table 1.

### 2.2 Model Development

Figure 1 shows the workflow for developing an interpretable model. The TCIA dataset was processed, with MRI data standardised to the Brain Imaging Data Structure (BIDS) format for consistency and reproducibility (Gorgolewski et al. 2016). Radiomics features were extracted, and the most discriminative features selected. These features trained various ML models to predict meningioma grade. SHAP was then applied for determining overall radiomics feature importance scores and model interpretation. The final model can predict meningioma grade in new cases.

#### 2.2.1 Image Processing and Radiomics Feature Extraction

The dataset had undergone a prior image processing pipeline, ensuring data consistency and quality. As detailed in (Vasantachart et al. 2022), anatomically co-registered T1C and T2 FLAIR MRI scans were obtained, with any misalignment corrected using the automated rigid registration software, VelocityAI. T2 FLAIR scans were resampled into their corresponding T1C scans, followed by isovoxel resampling. In the present study, further image processing techniques, including bias field correction and normalisation, were applied based on the

Table 1: Histopathological and demographic characteristics of the patients.

Features	Groups	Total	Female	Male
		94	67 (71.3%)	27 (28.7%)
Age	Min	25	25	29
	Mean	55.39	54.53	57.51
	Max	88	88	85
Grade	Low-grade	53 (56.4%)	46 (68.7%)	07 (26.0%)
	High-grade	41 (43.6%)	21 (31.3%)	20 (74.0%)
Location	Anterior and middle cranial fossa	45 (47.9%)	33 (49.3%)	12 (44.5%)
	Convexity	19 (20.2%)	09 (13.4%)	10 (37.0%)
	Falx and parasagittal	16 (17.0%)	12 (17.9%)	04 (14.8%)
	Posterior cranial fossa	12 (12.8%)	11 (16.4%)	01 (03.7%)
	Lateral ventricle	02 (02.1%)	02 (03.0%)	00 (00.0%)

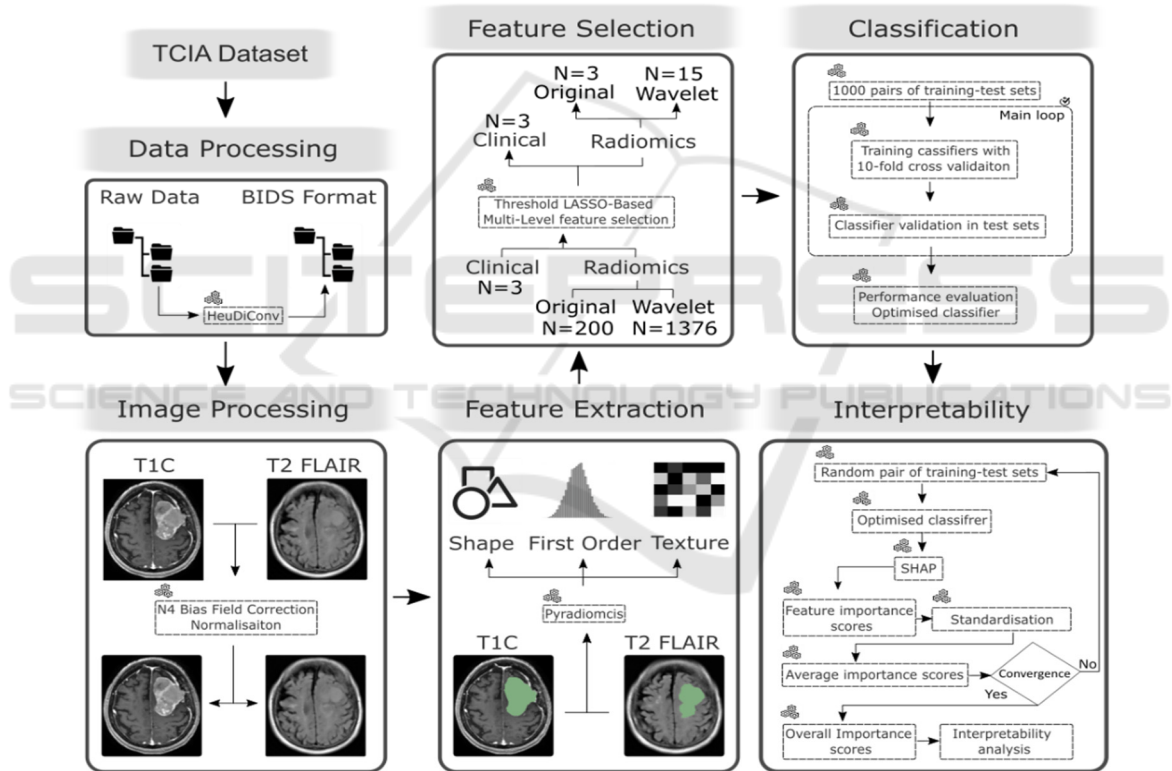


Figure 1: Study workflow.

radiomics standardisation protocol for brain MRI scans outlined in (Carré et al. 2020), using the SimpleITK N4BiasFieldCorrection and NormaliseImage filters (Yaniv et al. 2018). Manually delineated tumour lesions were also available within T1C and T2 FLAIR MRI scans. These annotations were created by a medical student and a radiation oncology resident and then reviewed by a radiation oncologist with over 5 years of experience

(Vasantachart et al. 2023). Radiomics features including shape, first-order, and texture features were subsequently extracted from these lesions.

### 2.2.2 Clinical and Radiomics Feature Selection

Feature selection is a key step in the development of ML models, as radiomics features often show strong

correlations, potentially resulting in redundant information, that can detrimentally affect model interpretability and generalisability (Reyes et al. 2020). LASSO, a widely used feature selection technique for analysing high-dimensional data, improves model performance and interpretation, although, highly correlated features may undermine its efficiency (Zou and Hastie 2003). To tackle this issue, we perform a multi-level feature selection method based on LASSO coefficient thresholds (Wang, An, et al. 2023). Clinical features were also analysed using the t-test for age and the chi-square test for gender and tumour location, with p-values below 0.05 as statistically significant.

### 2.2.3 ML Model to Classify Meningioma Grade

ML models for classifying low-grade and high-grade meningiomas were developed using LR, SVM, RF, and GB classifiers. To ensure robustness and generalisability, we conducted 1000 random training-test splits (1:4 ratio), generating training-test set pairs with 70 training and 24 test cases (An et al. 2021). Models were trained using 10-fold cross-validation within each training set. Model performance was evaluated by averaging AUC, Accuracy, Precision, Recall, and F1-score. The best-performing model was selected for interpretability analysis.

### 2.2.4 Model Interpretability

SHAP is a well-established technique for enhancing ML model interpretability. However, random perturbation-based sampling in SHAP implies that with different random seeds, a high ranked feature in one iteration may be considered as a low ranked feature in the next iteration (Xiang et al. 2023). To mitigate this issue, we determined overall radiomics feature importance scores by generating multiple training-test sets. The iteration process was terminated when the change in average importance scores for each feature was equal or less than 0.01 between two consecutive iterations. Overall radiomics feature importance scores were then considered as these averages. SHAP Kernel Explainer was utilised to determine radiomics feature importance scores in each iteration and scores were normalised by the sum of all feature importances.

### 2.2.5 Implementation

In this study, Python 3.8 was used for data conversion to BIDS format, image processing, radiomics feature extraction, and feature selection, as well as for ML

development, and interpretability analyses. The HeuDiConv tool (version 0.9.0, <https://github.com/nipy/heudiconv>), facilitated the conversion of DICOM files into BIDS format (Halchenko, Goncalves, and Castello 2020). Image processing was implemented using SimpleITK package (version 2.3.0). The open-source package Pyradiomics (version 3.1.0, <https://github.com/AIM-Harvard/pyradiomics>) was used for feature extraction (Van Griethuysen et al. 2017). Clinical categorical variables were encoded numerically. The Scikit-learn package (version 1.3.2) was used for radiomics feature selection, ML model development, and evaluation. Interpretability techniques was performed using SHAP (version 0.43.0) package.

## 3 RESULTS

### 3.1 Radiomics Feature Extraction

A total of 1576 radiomics features were extracted, including 14 shape features describing the size and contours of the tumours, 18 first-order features characterising the distribution of voxel intensities within the lesions, and 68 texture features measuring the variation of voxel intensities across T1C and T2 FLAIR MRI scans. Texture features were extracted using 22 Grey Level Co-occurrence Matrix (GLCM), 16 Gray-Level Run-length Matrix (GLRLM), 16 Gray-Level Size Zone Matrix (GLSZM), and 14 Gray Level Difference Matrix (GLDM). Subsequently, 688 wavelet radiomics features were evaluated by applying wavelet decomposition on the original images at both high and low frequencies.

### 3.2 Feature Selection and Model Performance

A subset of 18 radiomics features was identified as the most discriminative. Significant differences in age, gender, and tumour location between low-grade and high-grade meningiomas were observed, with p-values lower than 0.05. These clinical features were added to the radiomics subset to form a clinical-radiomics subset. The specifics of the feature subsets are outlined in Table 2, and the performance of ML models in training and test sets are shown in Table 3. The classifiers exhibited high accuracy and precision in distinguishing between tumour grades. Among the models, the SVM using the clinical-radiomics subset achieved the highest performance with AUC ( $0.90 \pm 0.12$  and  $0.83 \pm 0.07$ ), Accuracy ( $0.83 \pm 0.13$  and  $0.84 \pm 0.06$ ), Precision ( $0.84 \pm 0.18$  and  $0.82 \pm 0.10$ ), Recall

( $0.80 \pm 0.21$  and  $0.80 \pm 0.11$ ), and F1-score ( $0.80 \pm 0.16$  and  $0.80 \pm 0.08$ ) in training and test sets, respectively.

### 3.3 Model Interpretability

Figure 2 depicts overall radiomics feature importance scores. Figure 3 presents the SHAP violin summary plot, which illustrates the distribution and variability of SHAP values for each feature in distinguishing between low-grade and high-grade meningiomas. Higher SHAP values indicate greater impact on the model output, with wider violins showing higher density and more frequent values. Figure 4 represents feature SHAP dependence plots for the 3 top-ranked radiomics features. Figure 5 shows the interaction between the top-ranked radiomics feature with clinical features. In these figures each dot represents a prediction related to feature values, with the x-axis showing actual values and the y-axis showing SHAP values.

## 4 DISCUSSIONS

In this study, using clinical-radiomics feature subset, SVM model was the best-performing model with the highest average values of AUC ( $0.90 \pm 0.12$  and  $0.83 \pm 0.07$ ), Accuracy ( $0.83 \pm 0.13$  and  $0.84 \pm 0.06$ ), Precision ( $0.84 \pm 0.18$  and  $0.82 \pm 0.10$ ), Recall ( $0.80 \pm 0.21$  and  $0.80 \pm 0.11$ ), and F1-score ( $0.80 \pm 0.16$  and  $0.80 \pm 0.08$ ) in the training and test sets, respectively.

In the current study, the number of extracted radiomics features from T1C, and T2 FLAIR MRI scans was almost the same, highlighting the importance of using multi-parametric MRI scans in the relevant studies (Park, Shin, et al. 2022). Previous studies used clinical features and radiomics features from MRI scans to predict meningioma low-grade and high-grade. Duan et al. developed a radiomics nomogram with AUC of 0.95, using clinical and LASSO-selected radiomics features from T1C MRI scans (Duan, Zhou, et al. 2022). They also developed seven ML models, with the SVM model achieving an AUC of 0.88 (Duan, Li, et al. 2022). Similarly, Chu et al. used LASSO-selected radiomics features from T1, T1C, and T2 MRI scans to develop an LG model with an AUC of 0.95 (Chu et al. 2021). While these studies demonstrated strong predictive performance, they lacked interpretability in their models. Although complex machine learning models are effective in

capturing patterns in the data, they often result in models that are difficult for clinicians to interpret, where understanding the features influencing predictions is crucial for clinical management.

One major hinderance to the adoption of radiomics and ML models in the clinical management of meningiomas is the blackbox nature of ML models. To address this issue, SHAP was utilised to extract the overall radiomics feature importance scores and model interpretation. Here, GLRLM and GLSZM radiomics features were identified as the most discriminative features, showing high correlation with meningioma grade prediction (Han et al. 2021). GLSZM quantifies gray level zones within MRI scans. A gray level zone is defined as the number of connected voxels that share the same gray level intensity. GLRLM features describes heterogeneity in the distribution of run lengths (Traverso et al. 2020). The majority of selected radiomics features (15 out of 18) were derived from the wavelet-filtered MRI scans, which have been proved to be the most discriminative features in meningioma grade prediction (Han et al. 2021).

The violin plot depicted in Figure 3 indicates that higher values of the first radiomics feature, wavelet-HLH\_glszm\_ZoneEntropy\_t1c, correspond to an increased output probability of high-grade meningiomas. A similar trend was observed for the third radiomics feature, wavelet-LHL\_glszm\_GrayLevelNonUniformityNormalized\_t1c. Conversely, lower values of the second radiomics feature, wavelet-LHH\_glszm\_GrayLevelNonUniformityNormalized\_t2f, were associated with an increased output probability.

This study presented SHAP dependence plots to illustrate the 3 top-ranked radiomics feature interactions. The results presented in figure 4 a-c, show that (i) higher values of the first radiomics feature paired with lower values of the second increase the probability of high-grade meningiomas, while lower first feature values diminish this effect; (ii) lower values of the first feature combined with higher third feature values decrease probability, and (iii) the second feature values consistently impact probability regardless of the third feature values.

Interestingly, in this study, age emerged as a statistically significant feature in predicting meningioma grade based on t-test analysis. However, as depicted in the Figure 5.a, age does not exhibit a specific distribution that increases the output probability, aligning with (Hu et al. 2020; Duan, Li, et al. 2022).

Table 2: Total and statistically significant features.

Subset	Total features				Statistically significant features					
	Clinical	Radiomics		Clinical	Radiomics					
		Original	Wavelet		Original	Wavelet				
		T1C	T2 FLAIR		T1C	T2 FLAIR				
Radiomics	-	100	100	688	688	-	2	1	8	7
Clinical-Radiomics	3	100	100	688	688	3	2	1	8	7

Table 3: Prediction performance of ML models.

Classifier	Subset	Set	AUC	Accuracy	Precision	Recall	F1-Score
LR	radiomics	Training	0.83 ± 0.15	0.75 ± 0.14	0.73 ± 0.20	0.75 ± 0.23	0.72 ± 0.18
		Test	0.76 ± 0.08	0.76 ± 0.08	0.71 ± 0.11	0.77 ± 0.14	0.73 ± 0.09
	Clinical-radiomics	Training	0.88 ± 0.13	0.78 ± 0.14	0.78 ± 0.20	0.78 ± 0.22	0.75 ± 0.17
		Test	0.80 ± 0.08	0.80 ± 0.08	0.76 ± 0.11	0.79 ± 0.13	0.76 ± 0.09
SVM	radiomics	Training	0.87 ± 0.14	0.80 ± 0.20	0.81 ± 0.20	0.75 ± 0.24	0.75 ± 0.18
		Test	0.80 ± 0.07	0.80 ± 0.07	0.79 ± 0.11	0.75 ± 0.14	0.76 ± 0.09
	Clinical-radiomics	Training	0.90 ± 0.12	0.83 ± 0.13	0.84 ± 0.18	0.80 ± 0.21	0.80 ± 0.16
		Test	0.83 ± 0.07	0.84 ± 0.06	0.82 ± 0.10	0.80 ± 0.11	0.80 ± 0.08
RF	radiomics	Training	0.83 ± 0.15	0.76 ± 0.14	0.77 ± 0.22	0.72 ± 0.24	0.73 ± 0.20
		Test	0.76 ± 0.08	0.77 ± 0.08	0.73 ± 0.11	0.73 ± 0.14	0.72 ± 0.10
	Clinical-radiomics	Training	0.86 ± 0.14	0.78 ± 0.14	0.80 ± 0.21	0.72 ± 0.24	0.73 ± 0.19
		Test	0.77 ± 0.08	0.77 ± 0.08	0.75 ± 0.12	0.72 ± 0.14	0.72 ± 0.10
GB	radiomics	Training	0.79 ± 0.17	0.72 ± 0.15	0.71 ± 0.23	0.69 ± 0.24	0.67 ± 0.20
		Test	0.73 ± 0.09	0.73 ± 0.09	0.67 ± 0.10	0.71 ± 0.14	0.68 ± 0.10
	Clinical-radiomics	Training	0.79 ± 0.17	0.72 ± 0.15	0.70 ± 0.23	0.68 ± 0.25	0.67 ± 0.20
		Test	0.72 ± 0.08	0.72 ± 0.08	0.67 ± 0.11	0.69 ± 0.15	0.67 ± 0.10

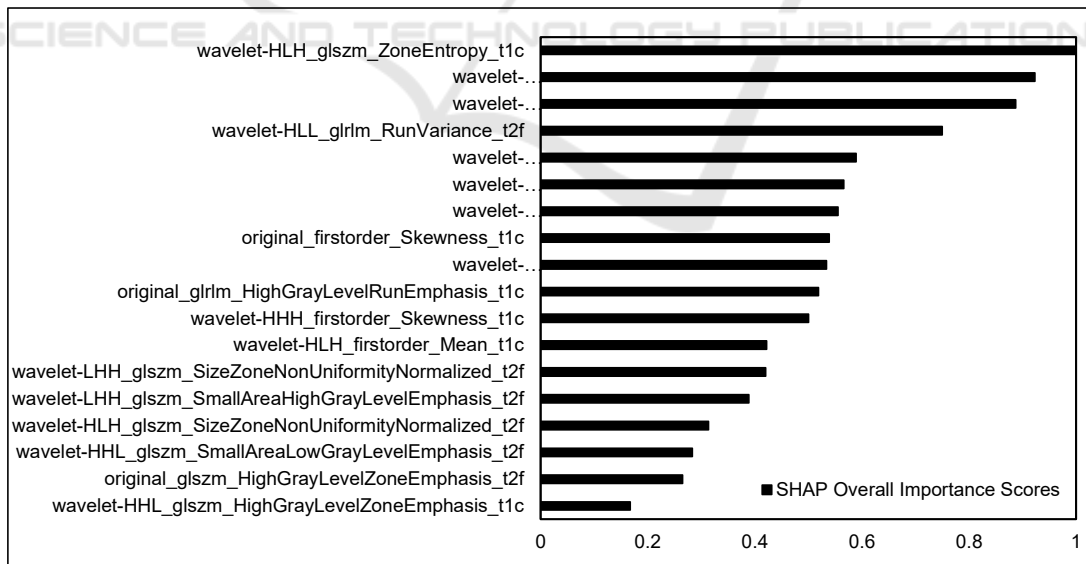


Figure 2: The overall radiomics feature importance scores of features extracted by SHAP. t1c: contrast-enhanced T1-weighted; t2f: T2-weighted fluid attenuated inversion recovery.

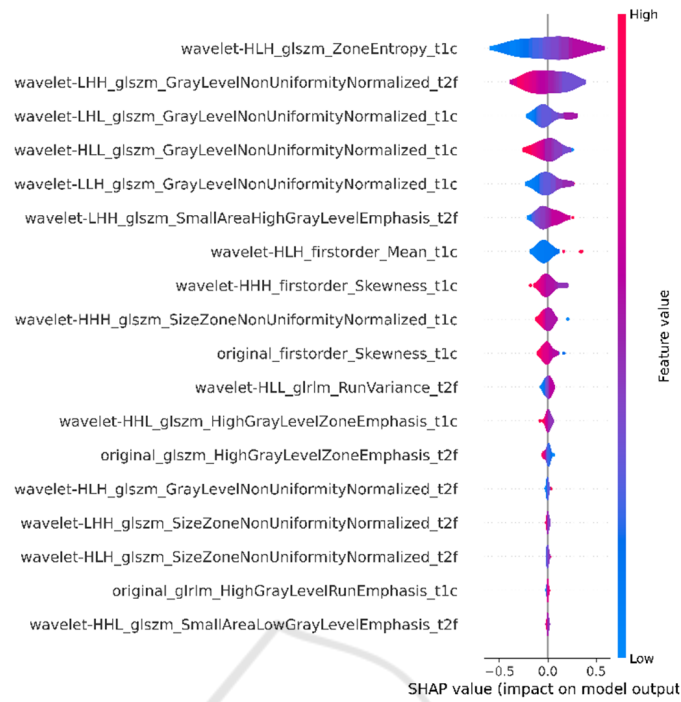


Figure 3: SHAP violin summary plot.

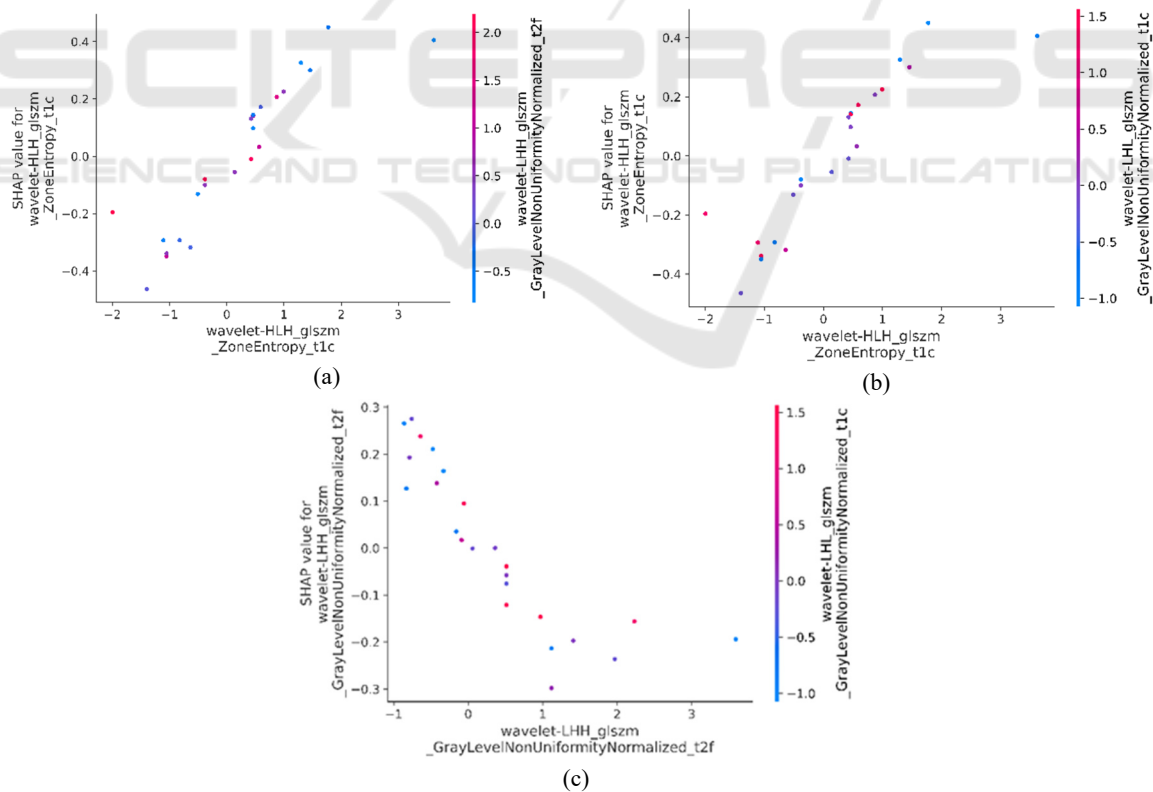


Figure 4: SHAP dependence plots for the three top-ranked radiomics features, illustrating the interactions between: (a) the first and second features, (b) the first and third features, and (c) the second and third features.

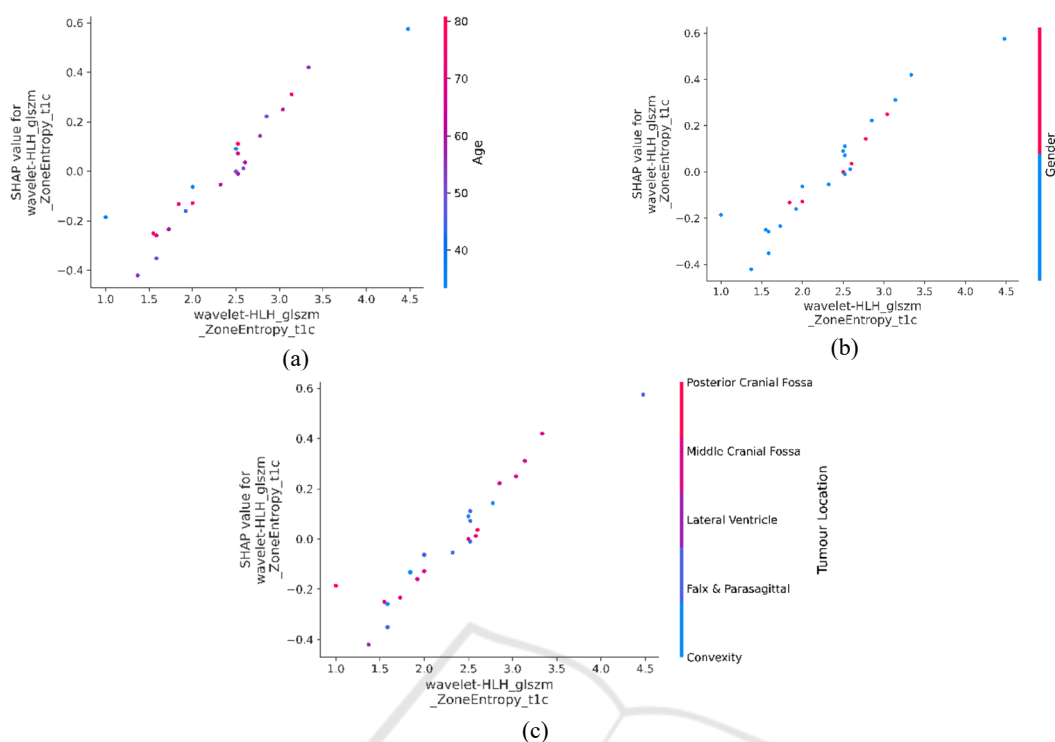


Figure 5: SHAP dependence plots for clinical and the top-ranked radiomics features, illustrating the interactions between the top-ranked radiomics features and: (a) age, (b) gender and (c) tumour location.

Conversely, concerning gender (as depicted in figure 5.b), males (red dots) show a tendency to decrease the output probability. Moreover, it is apparent that low values of the first radiomics feature in males, tend to decrease the output probability. This indicates that relying solely on statistical tests is not sufficiently reliable for predicting the effects of features on the model predictions. It was also shown that for females (blue dots), it generally increases the output probability while lower values of the first radiomics features tend to decrease the output probability.

Figure 5.c indicates that irrelevant to the tumour location, lower values of the first radiomics feature decrease the output probability while the combination of the posterior cranial fossa and middle cranial fossa locations and higher values of the first radiomics feature tends to increase the output probability.

When a new case is presented, our model helps clinicians to make better informed decisions by providing insights into the factors influencing predictions. Considering the interactions among radiomics features themselves and their interaction with clinical features may enable clinicians to consider additional nuances in their clinical judgments. Clinicians can also see which factors the model considers most critical, helping them understand the basis of the prediction. This also

enables comparison with previous cases. Clinicians can compare the new case with similar past cases where the model made predictions, seeing how the new case aligns or differs, thereby validating the model's prediction. Additionally, the model provides detailed explanations for each prediction, breaking down the contribution of each feature and offering a clear rationale that clinicians can review. It also helps identify anomalies. If a new case presents unusual patterns or outliers in the data, interpretable models can flag these anomalies, prompting further investigation by clinicians to ensure the prediction is accurate and relevant.

The current study has several limitations. TCIA, the publicly available dataset used here was retrospective, relatively small, and derived from a single institution. Grade III meningiomas were also excluded from the dataset due to their rare occurrence. However, leveraging public datasets provides researchers access to a diverse and extensive pool of medical imaging data, enabling robust analysis and enhancing the generalisability of findings across various patient populations and clinical strategies. Surprisingly, the utilisation of TCIA dataset accounts for only 4% in the meningiomas-relevant studies (Patel et al. 2023). This study only used two types of MRI scans while other MRI scans such as ADC mapping



were not considered. However, enhancing the clinical management of meningiomas by constructing an interpretable machine learning model that predicts meningioma grade was the main objective of this study.

## 5 CONCLUSIONS

Utilising clinical and radiomics features, the SVM ML model, offers a reliable approach for preoperative prediction of meningioma grade. By identifying discriminative radiomic features and their interactions with clinical features, SHAP supports the potential for the enhanced clinical adoption of such models. Future research should explore larger datasets and diverse patients to validate and refine these findings, further enhancing clinical adoption.

## REFERENCES

- An, Chansik, Yae Won Park, Sung Soo Ahn, Kyunghwa Han, Hwiyoung Kim, and Seung-Koo Lee. 2021. 'Radiomics machine learning study with a small sample size: Single random training-test set split may lead to unreliable results', *PLoS one*, 16: e0256152.
- Carré, Alexandre, Guillaume Klausner, Myriam Edjlali, Marvin Lerousseau, Jade Briend-Diop, Roger Sun, Samy Ammari, Sylvain Reuzé, Emilie Alvarez Andres, and Théo Estienne. 2020. 'Standardization of brain MR images across machines and protocols: bridging the gap for MRI-based radiomics', *Scientific reports*, 10: 12340.
- Chu, Hairui, Xiaoqi Lin, Jian He, Peipei Pang, Bing Fan, Pinggui Lei, Dongchuan Guo, and Chenglong Ye. 2021. 'Value of MRI radiomics based on enhanced T1WI images in prediction of meningiomas grade', *Academic radiology*, 28: 687-93.
- Clark, K., B. Vendt, K. Smith, J. Freymann, J. Kirby, P. Koppel, S. Moore, S. Phillips, D. Maffitt, M. Pringle, L. Tarbox, and F. Prior. 2013. 'The Cancer Imaging Archive (TCIA): maintaining and operating a public information repository', *J Digit Imaging*, 26: 1045-57.
- Duan, CF, N Li, Y Li, F Liu, JC Wang, XJ Liu, and WJ Xu. 2022. 'Comparison of different radiomic models based on enhanced T1-weighted images to predict the meningioma grade', *Clinical Radiology*, 77: e302-e07.
- Duan, Chongfeng, Xiaoming Zhou, Jiachen Wang, Nan Li, Fang Liu, Song Gao, Xuejun Liu, and Wenjian Xu. 2022. 'A radiomics nomogram for predicting the meningioma grade based on enhanced T1WI images', *The British Journal of Radiology*, 95: 20220141.
- Fountain, Daniel M., Adam M. H. Young, and Thomas Santarius. 2020. 'Chapter 24 - Malignant meningiomas.' in Michael W. McDermott (ed.), *Handbook of Clinical Neurology* (Elsevier).
- Gorgolewski, Krzysztof J, Tibor Auer, Vince D Calhoun, R Cameron Craddock, Samir Das, Eugene P Duff, Guillaume Flandin, Satrajit S Ghosh, Tristan Glatard, and Yaroslav O Halchenko. 2016. 'The brain imaging data structure, a format for organizing and describing outputs of neuroimaging experiments', *Scientific data*, 3: 1-9.
- Halchenko, Y, M Goncalves, and MVDO Castello. 2020. 'nipy/heudiconv v0.9.0', *Published online December*, 23.
- Han, Yuxuan, Tianzuo Wang, Peng Wu, Hao Zhang, Honghai Chen, and Chao Yang. 2021. 'Meningiomas: Preoperative predictive histopathological grading based on radiomics of MRI', *Magnetic Resonance Imaging*, 77: 36-43.
- Herrgott, Grayson A, James M Snyder, Ruicong She, Tathiane M Malta, Thais S Sabedot, Ian Y Lee, Jacob Pawloski, Guilherme G Podolsky-Gondim, Karam P Asmaro, and Jiaqi Zhang. 2023. 'Detection of diagnostic and prognostic methylation-based signatures in liquid biopsy specimens from patients with meningiomas', *Nature Communications*, 14: 5669.
- Hu, Jianping, Yijing Zhao, Mengcheng Li, Jianyi Liu, Feng Wang, Qiang Weng, Xingfu Wang, and Dairong Cao. 2020. 'Machine learning-based radiomics analysis in predicting the meningioma grade using multiparametric MRI', *European journal of radiology*, 131: 109251.
- Islim, Abdurrahman I, Midhun Mohan, Richard DC Moon, Nitika Rathi, Ruwanthi Kolamunnage-Dona, Anna Crofton, Brian J Haylock, Samantha J Mills, Andrew R Brodbelt, and Michael D Jenkinson. 2020. 'Treatment outcomes of incidental intracranial meningiomas: results from the IMPACT cohort', *World Neurosurgery*, 138: e725-e35.
- Jun, Yohan, Yae Won Park, Hyungseob Shin, Yejee Shin, Jeong Ryong Lee, Kyunghwa Han, Sung Soo Ahn, Soo Mee Lim, Dosik Hwang, and Seung-Koo Lee. 2023. 'Intelligent noninvasive meningioma grading with a fully automatic segmentation using interpretable multiparametric deep learning', *European radiology*: 1-10.
- Lambin, Philippe, Emmanuel Rios-Velazquez, Ralph Leijenaar, Sara Carvalho, Ruud GPM Van Stiphout, Patrick Granton, Catharina ML Zegers, Robert Gillies, Ronald Boellard, and André Dekker. 2012. 'Radiomics: extracting more information from medical images using advanced feature analysis', *European journal of cancer*, 48: 441-46.
- Langs, G, S Röhrich, J Hofmanninger, F Prayer, J Pan, C Herold, and H Prosch. 2018. 'Machine learning: from radiomics to discovery and routine', *Der Radiologe*, 58: 1.
- Louis, David N, Arie Perry, Pieter Wesseling, Daniel J Brat, Ian A Cree, Dominique Figarella-Branger, Cynthia Hawkins, HK Ng, Stefan M Pfister, and Guido Reifenberger. 2021. 'The 2021 WHO classification of tumors of the central nervous system: a summary', *Neuro-oncology*, 23: 1231-51.
- Low, Justin T, Quinn T Ostrom, Gino Cioffi, Corey Neff, Kristin A Waite, Carol Kruchko, and Jill S Barnholtz-Sloan. 2022. 'Primary brain and other central nervous system tumors in the United States (2014-2018): A

- summary of the CBTRUS statistical report for clinicians', *Neuro-oncology practice*, 9: 165-82.
- Park, Chae Jung, Seo Hee Choi, Jihwan Eom, Hwa Kyung Byun, Sung Soo Ahn, Jong Hee Chang, Se Hoon Kim, Seung-Koo Lee, Yae Won Park, and Hong In Yoon. 2022. 'An interpretable radiomics model to select patients for radiotherapy after surgery for WHO grade 2 meningiomas', *Radiation Oncology*, 17: 147.
- Park, Yae Won, Seo Jeong Shin, Jihwan Eom, Heirim Lee, Seng Chan You, Sung Soo Ahn, Soo Mee Lim, Rae Woong Park, and Seung-Koo Lee. 2022. 'Cycle-consistent adversarial networks improves generalizability of radiomics model in grading meningiomas on external validation', *Scientific reports*, 12: 7042.
- Patel, Ruchit V, Shun Yao, Raymond Y Huang, and Wenya Linda Bi. 2023. 'Application of radiomics to meningiomas: a systematic review', *Neuro-oncology*, 25: 1166-76.
- Reyes, Mauricio, Raphael Meier, Sérgio Pereira, Carlos A Silva, Fried-Michael Dahlweid, Hendrik von Tengg-Kobligk, Ronald M Summers, and Roland Wiest. 2020. 'On the interpretability of artificial intelligence in radiology: challenges and opportunities', *Radiology: artificial intelligence*, 2: e190043.
- Spille, Dorothee Caecilia, Peter B Sporns, Katharina Hess, Walter Stummer, and Benjamin Brokinkel. 2019. 'Prediction of high-grade histology and recurrence in meningiomas using routine preoperative magnetic resonance imaging: a systematic review', *World Neurosurgery*, 128: 174-81.
- Tagle, Patricio, Pablo Villanueva, Gonzalo Torrealba, and Isidro Huete. 2002. 'Intracranial metastasis or meningioma?: an uncommon clinical diagnostic dilemma', *Surgical neurology*, 58: 241-45.
- Traverso, Alberto, Michal Kazmierski, Ivan Zhovannik, Mattea Welch, Leonard Wee, David Jaffray, Andre Dekker, and Andrew Hope. 2020. 'Machine learning helps identifying volume-confounding effects in radiomics', *Physica Medica*, 71: 24-30.
- Van Griethuysen, Joost JM, Andriy Fedorov, Chintan Parmar, Ahmed Hosny, Nicole Aucoin, Vivek Narayan, Regina GH Beets-Tan, Jean-Christophe Fillion-Robin, Steve Pieper, and Hugo JW Aerts. 2017. 'Computational radiomics system to decode the radiographic phenotype', *Cancer research*, 77: e104-e07.
- Vassantachart, A., Cao, Y., Shen, Z., Cheng, K., Gribble, M., Ye, J. C., Zada, G., Hurth, K., Mathew. "Segmentation and Classification of Grade I and II Meningiomas from Magnetic Resonance Imaging: An Open Annotated Dataset (Meningioma-SEG-CLASS) (Version 1)." In, edited by The Cancer Imaging Archive.
- Vassantachart, April, Yufeng Cao, Michael Gribble, Samuel Guzman, Jason C Ye, Kyle Hurth, Anna Mathew, Gabriel Zada, Zhaoyang Fan, and Eric L Chang. 2022. 'Automatic differentiation of Grade I and II meningiomas on magnetic resonance image using an asymmetric convolutional neural network', *Scientific reports*, 12: 3806.
- Vassantachart, April, Yufeng Cao, Zhilei Shen, Karen Cheng, Michael Gribble, Jason C Ye, Gabriel Zada, Kyle Hurth, Anna Mathew, and Samuel Guzman. 2023. 'A repository of grade 1 and 2 meningioma MRIs in a public dataset for radiomics reproducibility tests', *Medical Physics*.
- Wang, Justin Z, Farshad Nassiri, Alexander P Landry, Vikas Patil, Jeff Liu, Kenneth Aldape, Andrew Gao, and Gelareh Zadeh. 2023. 'The multiomic landscape of meningiomas: a review and update', *Journal of Neuro-oncology*, 161: 405-14.
- Wang, Ke, Ying An, Jiancun Zhou, Yuehong Long, and Xianlai Chen. 2023. 'A novel Multi-Level feature selection method for radiomics', *Alexandria Engineering Journal*, 66: 993-99.
- Wang, Xiuying, Dingqian Wang, Zhigang Yao, Bowen Xin, Bao Wang, Chuanjin Lan, Yejun Qin, Shangchen Xu, Dazhong He, and Yingchao Liu. 2019. 'Machine learning models for multiparametric glioma grading with quantitative result interpretations', *Frontiers in neuroscience*, 12: 1046.
- Xiang, Xu, Hong Yu, Ye Wang, and Guoyin Wang. 2023. 'Stable local interpretable model-agnostic explanations based on a variational autoencoder', *Applied Intelligence*: 1-15.
- Yaniv, Ziv, Bradley C Lowekamp, Hans J Johnson, and Richard Beare. 2018. 'SimpleITK image-analysis notebooks: a collaborative environment for education and reproducible research', *Journal of digital imaging*, 31: 290-303.
- Zhang, Guobin, Yunsheng Zhang, Guijun Zhang, Da Li, Zhen Wu, Yonggang Wang, and Junting Zhang. 2019. 'Outcome and prognostic factors for atypical meningiomas after first recurrence', *Journal of Clinical Neuroscience*, 63: 100-05.
- Zhang, Jing, Kuan Yao, Panpan Liu, Zhenyu Liu, Tao Han, Zhiyong Zhao, Yuntai Cao, Guojin Zhang, Junting Zhang, and Jie Tian. 2020. 'A radiomics model for preoperative prediction of brain invasion in meningioma non-invasively based on MRI: A multicentre study', *EBioMedicine*, 58: 102933.
- Zou, Hui, and Trevor Hastie. 2003. 'Regression shrinkage and selection via the elastic net, with applications to microarrays', *JR Stat Soc Ser B*, 67: 301-20.